Journal of Solid Mechanics Vol. 13, No. 3 (2021) pp. 325-337
DOI: 10.22034/jsm.2020.1892727.1547

Thermoelastic Analysis of Annular Sector Plate Under Restricted Boundaries Amidst Elastic Reaction

A. Mahakalkar [1], V. Varghese [2,*]

[1]*Department of Mathematics, Mahatma Gandhi Science College, Armori, Gadchiroli, India*
[2]*Department of Mathematics, Smt. Sushilabai Bharti Science College, Arni, Yavatmal, India*

Received 10 June 2021; accepted 12 August 2021

ABSTRACT

An analytical framework is developed for the thermoelastic analysis of annular sector plate whose boundaries are subjected to elastic reactions. The exact expression for transient heat conduction with internal heat sources is obtained using a classical method. The fourth-order differential equation for the thermally induced deflection is obtained by developing a new integral transformation in accordance with the simply supported elastic supports that are subjected to elastic reactions. Here it is supposed that the movement of the boundaries is limited by an elastic reaction, that is, (a) shearing stress is proportional to the displacement, and (b) the reaction moment is proportional to the rate of change of displacement with respect to the radius. Finally, the maximum thermal stresses distributed linearly over the thickness of the plate are obtained in terms of resultant bending momentum per unit width. The calculation is obtained for the steel, aluminium and copper material plates using Bessel's function can be expressed in infinite series form, and the results are depicted using a few graphs.

Keywords: Heat conduction; Internal heat sources; Sector plate; Thermal deflection; Thermal stresses; integral transform.

1 INTRODUCTION

ALTHOUGH considerable attention has been given to the structural bending analysis and its associated thermal stress in a body due to its usage in different engineering application. It is also observed that the thermo-mechanical properties of the materials of which the structural profiles are made depend on the internal heat source and different broad temperature range of sectional heat supply. It further complicates the thermoelastic deflection solutions in connection with a different mode of supports which generates the nonlinearity of the system of equations, boundary conditions and so on. Therefore, few theoretical thermoelastic deflection studies on different structural objects with different supports have been investigated so far. For example, Khdeir and Reddy [1] investigated the thermoelastic bending response of cross-ply rectangular laminated plates using a higher-order theory and obtained the exact solutions using the state-space approach for different combinations of free, clamped, and simply supported edge conditions. Tsai and Hocheng [2] investigated the three-dimensional transient temperature heat conduction problem of the workpiece using the finite difference method, and the thermally-induced

*Corresponding author.
E-mail address: vino7997@gmail.com (V. Varghese)

deflection was analyzed by the numerical Simpson's 3/8 multiple integral methods. Kim and Noda [3] adopted Green's function approach for analyzing the deflection and the transient temperature distribution of a plate made of functionally graded materials by using the Galerkin method and the laminate theory. Green–Lagrange nonlinear strain-displacement relation was used by Na and Kim [4] for obtaining the thermoelastic deflection of functionally graded plates under uniform pressure and thermal load. Qian et al. [5] used the exact three-dimensional thermoelasticity theory to study the displacements and stresses in simply supported laminated rectangular plates within uniform temperature field, and it is observed that the numerical results agree well with the finite element solutions. Hasebe and Han [6] derived the thermoelastic thin-plate-bending solution for the elliptic hole under uniform bending heat flux using these Green's functions and the principle of superposition. Varghese et al. [7-11] have proposed various realistic thermoelastic-induced solutions for small and large deflection in the elliptic profile involving the Mathieu functions and also their derivatives using the classical method or integral techniques. Mirzaei [12] obtained the solution of thermal moments and buckling of the temperature-dependent composite plate, which is in a super elliptical profile reinforced with carbon nanotubes based on the Ritz method of the polynomial type. Very recently, Elsheikh et al. [13] obtained the closed-form solutions for the governing time-dependent heat conduction equation of the thin circular plate using Green's function method and variable separation technique. Past studies on the annular sector plates tend to be mostly limited to classical boundary conditions. It is widely believed that an accurate analytical solution is only feasible for an annular sector plate that is simply supported or clamped edges. However, many engineering applications usually encounter a variety of possible boundary conditions, such as restricted elastic reactions during edge movements. Therefore, as a result, such structural components are prone to deformations, bucking and bending for which proper analysis is required to be made when the boundary conditions are comprised of the involvement of elastic reactions that are generating during thermal expansion. It is also noted during the investigation that engineers and researchers are more interested in normal stress instead of shear stress since it is more prominent. However, there are cases in which the heat flow within a thin plate is considered for practical importance; in that case, the shear stress becomes more influential. Thus, the concept of shearing stress and reaction moment with the assumption that that the deflection of the plate is very small in comparison with its thickness will be of great interest to designers, engineers, scientists and researchers. Hence, to the best of authors' knowledge, there exists rare attentiveness on this topic of research in which displacement is taken into consideration for calculating bending stresses. The primary purpose of the current work is to take advantage of the movement of the boundaries restricted by an elastic reaction to fill this important gap in the problem of the plane stress field.

The article is organized as follows. In Section 2, the mathematical statement of the problem is presented. In Section 3, solutions of temperature distribution are expressed in terms of Bessel function and thermal-induced deflection is solved using a new integral transform. Section 4 is devoted to numerical analysis, and graphs are explained. Finally, some conclusions are drawn in Section 5. In Appendix Section, the calculus of the required integral transforms and its essential properties explained which is capable of solving the differential equation subjected to elastic reaction type boundary conditions.

2 FORMULATION OF THE PROBLEM

The geometry and cross-section in Fig. 1 show an annular sectoral plate composed of two radial and two circumferential edges within the cylindrical coordinate systems.

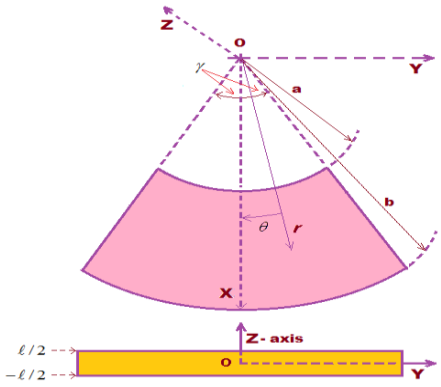

Fig.1
Geometry and dimensions of a sector plate and its cross-section.

The thin isotropic elastic plate is having a constant thickness ℓ, inner radius *a*, outer radius *b*, and sector angle 2γ. The plate geometry occupies the space D as $a \le r \le b, -\gamma \le \theta \le \gamma, -\ell/2 \le z \le \ell/2$, shown as a dark region in Fig. 1. The centre of the plate in the middle surface is taken as the origin.

2.1 Temperature distribution

The governing differential equation for the heat conduction with internal heat sources is given by

$$\frac{\partial^2 T}{\partial r^2}+\frac{1}{r}\frac{\partial T}{\partial r}+\frac{1}{r^2}\frac{\partial^2 T}{\partial \theta^2}+\frac{\partial^2 T}{\partial z^2}-\frac{1}{\kappa}\frac{\partial T}{\partial t}=-\frac{Q_0}{\kappa}f(t)g(r,\theta)\delta[z+(\ell/2)] \tag{1}$$

In which $T=T(r,\theta,z,t)$ is the temperature distribution in the thin plate, a ramp-type internal heat source as $Q=w_0/\rho C=(Q_0/\kappa)f(t)g(r,\theta)\delta[z+(\ell/2)]$ with w_0 as the quantity of heat generated by heat sources per unit time and volume, $g(r,\theta)$ is an assumed function of internal heat source, $\delta[\ ]$ is the Dirac delta function, thermal diffusivity is $\kappa = k/\rho C$, k being the conductivity, ρ is the material density, C is the specific heat of the material, respectively, and

$$\begin{aligned} f(t) &= (f_0/t_0)t \quad \text{for } 0 \le t \le t_0 \\ &= f_0 \qquad \text{for } \quad t > t_0 \end{aligned} \tag{2}$$

In which f_0 is constant and t_0 is a fixed time parameter. The initial condition and boundary conditions for temperature are

$$\begin{aligned} &T(r,\theta,z,t)\big|_{t=0}=0 \\ &T(r,\theta,z,t)\big|_{r=a}=0, T(r,\theta,z,t)\big|_{r=b}=0 \\ &T(r,\theta,z,t)\big|_{\theta=-\gamma}=0, T(r,\theta,z,t)\big|_{\theta=\gamma}=0 \\ &T(r,\theta,z,t)\big|_{z=-\ell/2}=0, T(r,\theta,z,t)\big|_{z=\ell/2}=0 \end{aligned} \tag{3}$$

2.2 Thermally-induced deflection

The thermally-induced deflection, dependent on the angle θ, governed by a differential equation

$$\frac{D}{2\rho\ell}\left(\frac{\partial^2}{\partial r^2}+\frac{1}{r}\frac{\partial}{\partial r}+\frac{1}{r^2}\frac{\partial^2}{\partial \theta^2}\right)^2 w(r,\theta,t)+\frac{\partial^2}{\partial t^2}w(r,\theta,t)=\frac{1}{1-\upsilon}F(r,\theta,t) \tag{4}$$

where $w(r,\theta,t)$ is the flexural displacement along the *z*-direction, *D* is the flexural rigidity of the plate given as $D = E\ell^3/12(1-\upsilon^2)$, inertia loading term is taken as $\rho\ell(\partial^2 w/\partial t^2)$, ρ is the mass density, $M_T(r,\theta,t)$ is the thermally induced resultant moment as:

$$M_T(r,\theta,t)=\alpha E\int_{-\ell/2}^{\ell/2} z\,T(r,\theta,z,t)dz \tag{5}$$

and

$$F(r,\theta,t)=\left(\frac{\partial^2}{\partial r^2}+\frac{1}{r}\frac{\partial}{\partial r}+\frac{1}{r^2}\frac{\partial^2}{\partial \theta^2}\right)M_T(r,\theta,t)$$

with α and E symbolize as the coefficient of linear thermal expansion and Young's Modulus of the material of the plate, respectively. The initial boundary conditions are given as:

$$w(r,\theta,t)\big|_{t=0} = f(r,\theta),\ \frac{\partial}{\partial t} w(r,\theta,t)\bigg|_{t=0} = h(r,\theta) \tag{6}$$

In which $f(r,\theta)$ and $h(r,\theta)$ are the assumed functions. Marchi and Diaz [14,15] treated axisymmetric vibration of annular plates by means of the integral-transform method, and the method was extended to a plate with elastic edge conditions. We shall suppose that the movement of simply supported boundaries at $r=a$ and $r=b$ is limited by an elastic reaction. Therefore, $w(r,\theta,t)$ shall satisfy the boundary conditions as:

$$\left.\begin{aligned} \left(\frac{\partial^3}{\partial r^3} - \frac{1}{r^2}\frac{\partial}{\partial r} + \frac{1}{r}\frac{\partial^2}{\partial r^2}\right) w(r,\theta,t)\bigg|_{r=a\,\text{or}\,b} &= -k_1 w(r,\theta,t)\big|_{a\,\text{or}\,b} \\ \left(\frac{\partial^2}{\partial r^2} + \frac{1}{r}\frac{\partial}{\partial r}\right) w(r,\theta,t)\bigg|_{r=a\,\text{or}\,b} &= -k_2 \frac{\partial}{\partial r} w(r,\theta,t)\bigg|_{a\,\text{or}\,b} \end{aligned}\right\} \tag{7}$$

where w is the flexural displacement, $\partial w/\partial r$ is the rate of change of displacement with respect to the radius, $\partial^3 w/\partial r^3 - (1/r^2)\partial w/\partial r + (1/r)\partial^2 w/\partial r^2$ [16] is the shearing stress, $\partial^2 w/\partial r^2 + (1/r)\partial w/\partial r$ [17] is the reaction moment, and both the proportionality constants k_1 and k_2 depend on the thermoelastic properties of the surrounding medium, respectively.

The classical homogeneous boundary conditions can be simply considered as special cases when the elastic reactions are considered as zero.

2.3 Thermally induced stresses

The thermal bending stresses components over the thickness of the plate is expressed as:

$$\sigma_{rr} = \frac{M_{rr}}{(\ell^2/6)}\left(\frac{z}{\ell/2}\right), \sigma_{\theta\theta} = \frac{M_{\theta\theta}}{(\ell^2/6)}\left(\frac{z}{\ell/2}\right), \sigma_{r\theta} = \frac{M_{r\theta}}{(\ell^2/6)}\left(\frac{z}{\ell/2}\right) \tag{8}$$

In which resultant bending momentum per unit length [17] is

$$\begin{aligned} M_{rr} &= -D\left\{\frac{\partial^2 w}{\partial r^2} + \upsilon\left(\frac{1}{r}\frac{\partial w}{\partial r} + \frac{1}{r^2}\frac{\partial^2 w}{\partial \theta^2}\right)\right\} - \frac{M_T}{1-\upsilon}, \\ M_{\theta\theta} &= -D\left\{\upsilon\frac{\partial^2 w}{\partial r^2} + \left(\frac{1}{r}\frac{\partial w}{\partial r} + \frac{1}{r^2}\frac{\partial^2 w}{\partial \theta^2}\right)\right\} - \frac{M_T}{1-\upsilon} \\ M_{r\theta} &= D(1-\upsilon)\frac{1}{r}\frac{\partial^2 w}{\partial r\,\partial \theta} \end{aligned} \tag{9}$$

Eqs. (1) to (9) constitutes the mathematical formulation of the problem under consideration.

3 THE SOLUTION TO THE PROBLEM

3.1 Solution for the temperature distribution

Applying the Laplace transform of Eq. (1), one obtains

$$\frac{\partial^2 \bar{T}}{\partial r^2}+\frac{1}{r}\frac{\partial \bar{T}}{\partial r}+\frac{1}{r^2}\frac{\partial^2 \bar{T}}{\partial \theta^2}+\frac{\partial^2 \bar{T}}{\partial z^2}-\frac{p}{\kappa}\bar{T}=-\frac{Q_0 f_0}{\kappa t_0}(1-e^{-t_0 p})g(r,\theta)\delta[z+(\ell/2)] \tag{10}$$

with

$$\begin{aligned}
&\bar{T}(r,\theta,z,p)\big|_{r=a}=0, \bar{T}(r,\theta,z,p)\big|_{r=b}=0\\
&\bar{T}(r,\theta,z,p)\big|_{\theta=-\gamma}=0, \bar{T}(r,\theta,z,p)\big|_{\theta=\gamma}=0\\
&\bar{T}(r,\theta,z,p)\big|_{z=-\ell/2}=0, \bar{T}(r,\theta,z,p)\big|_{z=\ell/2}=0
\end{aligned} \tag{11}$$

In which $\bar{T}$ is the transformed function of T, and p is transformed Laplace parameter. As a solution of Eq. (10) satisfying Eq. (11), we assume

$$\bar{T}(r,\theta,z,p)=\sum_{t=1}^{\infty}\sum_{s=1}^{\infty}A_{ms}\sin m\theta C_m(\alpha_{ms}r)\sinh\{\gamma_{ms}[z+(\ell/2)]\} \tag{12}$$

In which A_{ms} is the constant to be determined from boundary conditions and $C_m(\alpha_{ms}r)$ denotes a cylinder function of order m as:

$$C_m(\alpha_{ms}r)=J_m(\alpha_{ms}r)-\varepsilon_{ms}Y_m(\alpha_{ms}r) \tag{13}$$

where $\varepsilon_{ms}=\dfrac{J_m(\alpha_{ms}a)}{Y_m(\alpha_{ms}a)}$ for $m=\dfrac{n\pi}{\gamma}$ $(n=1,3,..)$, $\alpha_{ms}=\dfrac{\lambda_{ms}}{a}$ $(s=1,2,..)$ with $J_m(\alpha_{ms}r)$ and $Y_m(\alpha_{ms}r)$ as the Bessel function of first and second kind of order m. From boundary condition (11) on $r=b$, we have λ_{ms} as the roots of the transcendental equation $J_m(\lambda_{ms}\wp)Y_m(\lambda_{ms})-J_m(\lambda_{ms})Y_m(\lambda_{ms}\wp)=0$, $\wp=b/a$. The boundary conditions (11) on $r=a, \theta=\pm\gamma, z=-\ell/2$ is already satisfied in Eq. (13), and γ_{ms} is obtained from Eq. (10) with the aid of Eq. (10) as $\gamma_{ms}=[\alpha_{ms}^2+(p/\kappa)]^{1/2}$.

As the solution (12) satisfies the conditions of Eq. (11), we assume the function $g(r,\theta)$ in terms of Fourier-Bessel series as:

$$g(r,\theta)=\sum_{n=1}^{\infty}\sum_{s=1}^{\infty}f_{ns}C_m(\alpha_{ms}r)\sin m\theta \tag{14}$$

In which

$$f_{ns}=\frac{\int_{-\gamma}^{\gamma}\int_a^b g(r,\theta)\,r\,C_m(\alpha_{ms}r)\sin m\theta\,dr\,d\theta}{\int_{-\gamma}^{\gamma}\sin^2 m\theta\,d\theta\int_a^b r[C_m(\alpha_{ms}r)]^2\,dr} \tag{15}$$

Using Eqs. (12) and (14) gives a relation between f_{ns} and A_{ms} as:

$$A_{ms}=-\frac{Q_0 f_0}{\kappa t_0}\left[\frac{1-e^{-t_0 p}}{\gamma_{ms}^2-(p/\kappa)}\right]f_{ns} \tag{16}$$

Then the Eq. (12) with the aid of Eq. (16), yields

$$\bar{T}(r,\theta,z,p) = -\frac{Q_0 f_0}{\kappa t_0}\sum_{t=1}^{\infty}\sum_{s=1}^{\infty}\left[\frac{1-e^{-t_0 p}}{\gamma_{ms}^2-(p/\kappa)}\right] f_{ns}\sin m\theta C_m(\alpha_{ms}r)\delta[z+(\ell/2)] \tag{17}$$

Inverting Eq. (17) by Laplace inversion theorem, the temperature field is obtained as:

$$T = \frac{Q_0 f_0}{t_0}\sum_{t=1}^{\infty}\sum_{s=1}^{\infty} f_{ns}\sin m\theta C_m(\alpha_{ms}r)\delta[z+(\ell/2)]e^{\gamma_{ms}^2\kappa t}\left[1-e^{(t-t_0)\gamma_{ms}^2\kappa}H(t-t_0)\right] \tag{18}$$

The function is given in Eq. (18) represents the temperature $T(r,\theta,z,t)$ at every instance and at all point of the thin annular sector plate with a finite height when there are conditions of heat contour acting on surfaces $r=a,\ r=b,\ z=-\ell/2,\ z=\ell/2,$ and when on the faces $\theta=-\gamma,\ \theta=\gamma$ the temperatures are reached.

3.2 Solution for thermal deflection

Putting Eq. (18) in Eq. (5), one obtains

$$M_T = \frac{\alpha E Q_0 f_0}{t_0}\sum_{t=1}^{\infty}\sum_{s=1}^{\infty} f_{ns}\sin m\theta C_m(\alpha_{ms}r)[\ell(1-2H(\ell))/2]e^{\gamma_{ms}^2\kappa t}\times\left[1-e^{(t-t_0)\gamma_{ms}^2\kappa}H(t-t_0)\right] \tag{19}$$

By means of a new integral transform (refer Appendix) over the variable *r* and taking into account the boundary conditions (7), the Eq. (4) is transformed into

$$\frac{D}{2\rho\ell}\xi_j^4\bar{w}(\xi_j,\theta,t)+\frac{\partial^2}{\partial t^2}\bar{w}(\xi_j,\theta,t) = \frac{1}{1-\upsilon}\bar{F}(\xi,\theta,t) \tag{20}$$

In which

$$\bar{F}(\xi,\theta,t) = \int_a^b\int_0^{2\pi} r\left[\left(\frac{\partial^2}{\partial r^2}+\frac{1}{r}\frac{\partial}{\partial r}+\frac{1}{r^2}\frac{\partial^2}{\partial\theta^2}\right)M_T(r,\theta,t)\right]X_0(k_1,k_2,\xi_j r,\theta)\,dr\,d\theta$$

Using the Laplace transform, the differential Eq. (20) taking into account the initial conditions (6), one yield

$$\bar{\bar{w}}(\xi_j,\theta,s) = \frac{\bar{\bar{F}}(\xi_j,\theta,s)}{(1-\upsilon)(\Phi\xi_j^4+s^2)}+\frac{s\bar{f}(\xi_j,\theta)}{(\Phi\xi_j^4+s^2)}+\frac{\bar{h}(\xi_j,\theta)}{(\Phi\xi_j^4+s^2)} \tag{21}$$

In which $\Phi = D/2\rho\ell$. Now taking Laplace inverse transform and then taking the inverse of the new integral transform (refer Appendix), one obtains the solution of thermal deflection as:

$$\begin{aligned} w(r,\theta,t) = \sum_{j|\xi_j>0}\sum_{m=1}^{\infty}\frac{1}{\gamma_j}\Bigg\{&\bar{f}(\xi_j,\theta)\cos(\sqrt{\Phi}\xi_j^2 t)+\frac{\bar{h}(\xi_j,\theta)}{\sqrt{\Phi}\xi_j^2}\sin(\sqrt{\Phi}\xi_j^2 t)\\ &+\frac{1}{(1-\upsilon)\sqrt{\Phi}\xi_j^2}\int_0^t\bar{F}(\xi_j,\theta,\tau)\sin[\sqrt{\Phi}\xi_j^2(t-\tau)]d\tau\Bigg\}X_0(k_1,k_2,\xi_j r,\theta)\end{aligned} \tag{22}$$

3.3 Solution for bending moments

On substituting Eq. (22) in Eq. (9), one obtains the resultant bending momentum as:

$$M_{rr}=\frac{D\ \sin(m\theta)}{12\,t(\vartheta-1)}\Big\langle -e^{1+(2t-t_0)\gamma_{ms}^2\kappa}\overline{f}(\xi_j,\theta)f_{ns}Q_0\alpha E\,\ell^3[J_m(\alpha_{ms}r)$$
$$-\varepsilon_{ms}Y_m(\alpha_{ms}r)]H(t-t_0)+\frac{1}{r^2}\Big\{e^{1+t\gamma_{ms}^2\kappa}\overline{f}(\xi_j,\theta)f_{ns}Q_0\alpha\ell^3$$
$$\times[J_m(\alpha_{ms}r)-\varepsilon_{ms}Y_m(\alpha_{ms}r)]-12\,t(\vartheta-1)\{-m^2\vartheta[J_0(\xi_j r)$$
$$+I_0(\xi_j r)+K_0(\xi_j r)-Y_0(\xi_j r)]+\xi_j r[(-\vartheta+1)[-J_1(\xi_j r)$$
$$+I_1(\xi_j r)+K_1(\xi_j r)+Y_1(\xi_j r)]+[-J_0(\xi_j r)+I_0(\xi_j r)$$
$$+K_0(\xi_j r)+Y_0(\xi_j r)]\xi_j]\}+1/\gamma[\overline{f}(\xi_j,\theta)\cos(\sqrt{\Phi}\xi_j^2 t)$$
$$+\frac{\overline{F}(\xi_j,\theta,t_1)(\cos\sqrt{\Phi}\xi_j^2(t-t_1)-\cos\sqrt{\Phi}\xi_j^2 t)}{(-1+\upsilon)\Phi\xi_j^4}+\frac{g(r,\theta)\sin(\sqrt{\Phi}\xi_j^2 t)}{\sqrt{\Phi}\xi_j^2}\Big\}\Big\rangle \tag{23}$$

$$M_{\theta\theta}=\frac{-D\ \sin(m\theta)}{2}\Big\langle\ [2\overline{f}(\xi_j,\theta)f_{ns}Q_0\alpha E[J_m(\alpha_{ms}r)-\varepsilon_{ms}Y_m(\alpha_{ms}r]$$
$$\times(1-e^{(2t-t_0)\gamma_{ms}^2\kappa}H(t-t_0))]\ell^3e^{t\gamma_{ms}^2\kappa}/t(\upsilon-1)]-\Big\{\frac{2m^2}{r^2}(J_0(\xi_j r)+I_0(\xi_j r)+K_0(\xi_j r)-Y_0(\xi_j r))$$
$$-2\xi_j/r[(-\vartheta+1)(-J_1(\xi_j r)+I_1(\xi_j r)+K_1(\xi_j r)+Y_1(\xi_j r))$$
$$-\upsilon\xi_j[-J_0(\xi_j r)+J_2(\xi_j r)+I_0(\xi_j r)+I_2(\xi_j r)+K_0(\xi_j r)+K_2(\xi_j r)+Y_0(\xi_j r)-Y_2(\xi_j r)]\Big\}$$
$$\times1/\gamma[\overline{f}(\xi_j,\theta)\cos(\sqrt{\Phi}\xi_j^2 t)+1/\gamma[\overline{f}(\xi_j,\theta)\cos(\sqrt{\Phi}\xi_j^2 t)$$
$$+\frac{\overline{F}(\xi_j,\theta,t_1)(\cos\sqrt{\Phi}\xi_j^2(t-t_1)-\cos\sqrt{\Phi}\xi_j^2 t)}{(-1+\upsilon)\Phi\xi_j^4}+\frac{g(r,\theta)\sin(\sqrt{\Phi}\xi_j^2 t)}{\sqrt{\Phi}\xi_j^2}\Big\}\Big\rangle \tag{24}$$

$$M_{r\theta}=\frac{D\ m(1-\upsilon)}{r^2}\Big\langle\ [-J_1(\xi_j r)+I_1(\xi_j r)-K_1(\xi_j r)+Y_1(\xi_j r)]\times\cos(\theta\xi_j)+1/\gamma\Big\{\ \overline{f}(\xi_j,\theta)\cos(\sqrt{\Phi}\xi_j^2 t)$$
$$+\frac{\overline{F}(\xi_j,\theta,t_1)(\cos\sqrt{\Phi}\xi_j^2(t-t_1)-\cos\sqrt{\Phi}\xi_j^2 t)}{(-1+\upsilon)\Phi\xi_j^4}+\frac{g(r,\theta)\sin(\sqrt{\Phi}\xi_j^2 t)}{\sqrt{\Phi}\xi_j^2}\Big\}\Big\rangle \tag{25}$$

3.4 Solution for the associated stresses

Now using Eqs. (23)-(25) in Eq. (8), one obtains the associated stresses expressions as:

$$(\sigma_{rr})_{max}=\frac{Dz\ \sin(m\theta)}{\ell^3 t(\vartheta-1)}\Big\langle\ -e^{(2t-t_0)\gamma_{ms}^2\kappa}\overline{f}(\xi_j,\theta)f_{ns}Q_0\alpha E\,\ell^3[J_m(\alpha_{ms}r)$$
$$-\varepsilon_{ms}Y_m(\alpha_{ms}r)H(t-t_0)+\frac{1}{r^2}\Big\{e^{1+t\gamma_{ms}^2\kappa}\overline{f}(\xi_j,\theta)f_{ns}Q_0\alpha\ell^3$$
$$\times[J_m(\alpha_{ms}r)-\varepsilon_{ms}Y_m(\alpha_{ms}r)]-12\,t(\vartheta-1)\{-m^2\vartheta[J_0(\xi_j r)$$
$$+I_0(\xi_j r)+K_0(\xi_j r)-Y_0(\xi_j r)]+\xi_j r[(-\vartheta+1)[-J_1(\xi_j r)$$
$$+I_1(\xi_j r)+K_1(\xi_j r)+Y_1(\xi_j r)]+[-J_0(\xi_j r)+I_0(\xi_j r)+K_0(\xi_j r)$$
$$+Y_0(\xi_j r)]\xi_j]\}+1/\gamma[\overline{f}(\xi_j,\theta)\cos(\sqrt{\Phi}\xi_j^2 t)$$
$$+\frac{\overline{F}(\xi_j,\theta,t_1)(\cos\sqrt{\Phi}\xi_j^2(t-t_1)-\cos\sqrt{\Phi}\xi_j^2 t)}{(-1+\upsilon)\Phi\xi_j^4}+\frac{g(r,\theta)\sin(\sqrt{\Phi}\xi_j^2 t)}{\sqrt{\Phi}\xi_j^2}\Big\}\Big\rangle \tag{26}$$

$$
\begin{aligned}
(\sigma_{\theta\theta})_{max} = \frac{-6Dz\ \sin(m\theta)}{\ell^3}\Bigg\langle\ & [2\bar{f}\,(\xi_j,\theta) f_{ns} Q_0 \alpha E [J_m(\alpha_{ms} r) - \varepsilon_{ms} Y_m(\alpha_{ms} r] \\
& \times (1 - e^{(2t-t_0)\gamma_{ms}^2 \kappa} H(t-t_0))]\ell^3 e^{t\gamma_{ms}^2\kappa}/t(\upsilon-1)] - \Bigg\{\frac{2m^2}{r^2}(J_0(\xi_j r) + I_0(\xi_j r) + K_0(\xi_j r) - Y_0(\xi_j r)) \\
& - 2\xi_j / r[(-\vartheta+1)(-J_1(\xi_j r) + I_1(\xi_j r) + K_1(\xi_j r) + Y_1(\xi_j r)) \\
& - \upsilon\xi_j [-J_0(\xi_j r) + J_2(\xi_j r) + I_0(\xi_j r) + I_2(\xi_j r) + K_0(\xi_j r) + K_2(\xi_j r) + Y_0(\xi_j r) - Y_2(\xi_j r)]\Bigg\} \\
& \times 1/\gamma[\bar{f}\,(\xi_j,\theta)\cos(\sqrt{\Phi}\xi_j^2 t) + 1/\gamma[\bar{f}\,(\xi_j,\theta)\cos(\sqrt{\Phi}\xi_j^2 t) \\
& + \frac{\bar{F}(\xi_j,\theta,t_1)(\cos\sqrt{\Phi}\xi_j^2(t-t_1) - \cos\sqrt{\Phi}\xi_j^2 t)}{(-1+\upsilon)\Phi\xi_j^4} + \frac{g(r,\theta)\sin(\sqrt{\Phi}\xi_j^2 t)}{\sqrt{\Phi}\xi_j^2}\Bigg\}\Bigg\rangle
\end{aligned}
\tag{27}
$$

$$
\begin{aligned}
(\sigma_{r\theta})_{max} = \frac{12zD\ m(1-\upsilon)}{\ell^3 r^2}\Big\langle & [-J_1(\xi_j r) + I_1(\xi_j r) - K_1(\xi_j r) + Y_1(\xi_j r)] \\
& \times \cos(\theta\xi_j) + 1/\gamma\Big\{\bar{f}\,(\xi_j,\theta)\cos(\sqrt{\Phi}\xi_j^2 t) \\
& + \frac{\bar{F}(\xi_j,\theta,t_1)(\cos\sqrt{\Phi}\xi_j^2(t-t_1) - \cos\sqrt{\Phi}\xi_j^2 t)}{(-1+\upsilon)\Phi\xi_j^4} + \frac{g(r,\theta)\sin(\sqrt{\Phi}\xi_j^2 t)}{\sqrt{\Phi}\xi_j^2}\Big\}\Big\rangle
\end{aligned}
\tag{28}
$$

4 NUMERICAL RESULTS , DISCUSSION AND REMARKS

For the interests of the simplicity of calculation, we introduce the following dimensionless values

$$
\begin{aligned}
& \bar{r} = r/b,\ \bar{z} = [z - (-\ell/2)]/b,\ \tau = \kappa t/b^2, \bar{T} = T/T_0, \\
& \bar{w} = w/\alpha T_0 b, \bar{\sigma}_{ij} = \sigma_{ij}/E\alpha T_0 (i,j = r,\theta), \bar{M}_{ij} = M_{ij}/Eb^3
\end{aligned}
\tag{29}
$$

Substituting the above Eq. (29) into Eqs. (18), (22), one obtains the expressions for the dimensionless temperature, deflection and thermal stresses respectively for our numerical discussion. The thermo-mechanical properties are considered as specific heat at constant pressure as shown in Table 1.

Table 1
Thermo-mechanical properties at room temperature.

Parameters	Units	Copper	Aluminium	Steel
Calorific value	*Kcal/Kg^{0}C*	0.092	0.22	0.049
Modulus of Elasticity	*Gpa*	110	70	190
Shear Modulus	*GPa*	45	27	80
Poisson Ratio		0.34	0.33	0.29
Thermal Expansion coefficient	10 $^{-6}$ *m/m^{0}C*	17.6	23.6	11.5
Thermal Conductivity	*W/mK*	401	237	51.9
Density	*Kg/m^3*	8940	2712	7870
Thermal Diffusivity	*m^2/s*	1.11 × 10^{-5}	9.7 × 10^{-5}	1.88 × 10^{-5}

The physical parameter for the sector plate is considered as $a = 0.2m,\ b = 1m,\ \ell = 0.08m,\ t_0 = 0.3$ and $T_0 = 150^{\circ}C$. Considering the initial boundary conditions of the thermally-induced deflection as $f(r,\theta) = 0,\ h(r,\theta) = 0$ and the internal source term which is partially constant in the *r*- direction and which follows a quadratic parabola in the $\theta-$ direction

$$g(r,\theta)=\begin{cases} T_0(1/\gamma)^2[\gamma^2-\theta^2] \text{ for } \dfrac{a+b-c}{2}<r<\dfrac{a+b+c}{2} \text{ and } -\gamma\le\theta\le\gamma \\ 0 \qquad \text{for } a\le r<\dfrac{a+b-c}{2} \text{ or } \dfrac{a+b+c}{2}<r\le b \text{ and } -\gamma\le\theta\le\gamma \end{cases} \tag{30}$$

where y -intercept of the equation is c. The $\alpha_{ms}=0.529,\ 0.679,\ 0.826,\ 0.977,\ 1.129,\ 1.282,\ 1.436,\ 1.599,\ 1.746,\ 1.902,\ldots$ are the roots of the transcendental equation $C_m(\alpha_{ms}r)=J_m(\alpha_{ms}r)-[J_m(\alpha_{ms}a)/Y_m(\alpha_{ms}a)]Y_m(\alpha_{ms}r)$. Numerical results were obtained by taking the first 10 terms for n in an odd number and 48 terms for s in the series. In order to examine the influence of internal heat generation on the plate, the numerical calculations were performed for all the variables, and numerical calculations are depicted in the following figures with the help of Mathematica software. Fig.2-4 analyzed the numerical results of the temperature distribution, thermal deflection and thermal stresses in the annular sector plate under the action of a ramp-type quadratic parabola internal heat source.

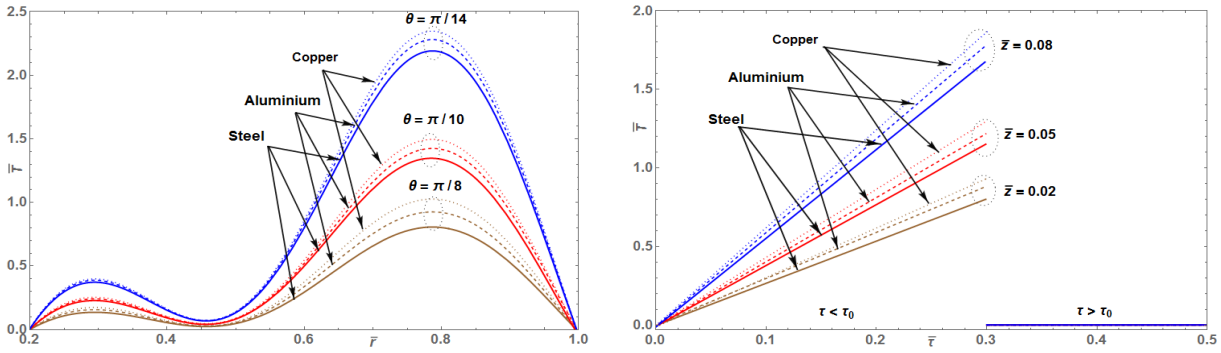

(a) (b)

Fig.2

a) Temperature distribution along $\bar{r}$ -direction for different values of θ. b)Temperature distribution along time for different values of $\bar{z}$.

Fig 2(a) represents the analysis of temperature distribution along the radial direction for the various angles. Since the plate is subjected to a compressive force acting along the inner edge, the maximum temperature distribution attains at the outer edge. The variation in the temperature distribution may be due to the available ramp-type internal source term which is partially constant in the $r-$direction and which follows a quadratic parabola in the $\theta-$direction. Fig. 2(b) notify variation in the temperature distribution along the time-invariant. It is observed that temperature distribution varies directly with respect time. It is understood from the figure that the temperature is zero initially and goes on increasing linearly with time up to a certain interval. It is also to be noticed that the temperature suddenly drops to zero and becomes steady due to the relation $\tau>\tau_0$.

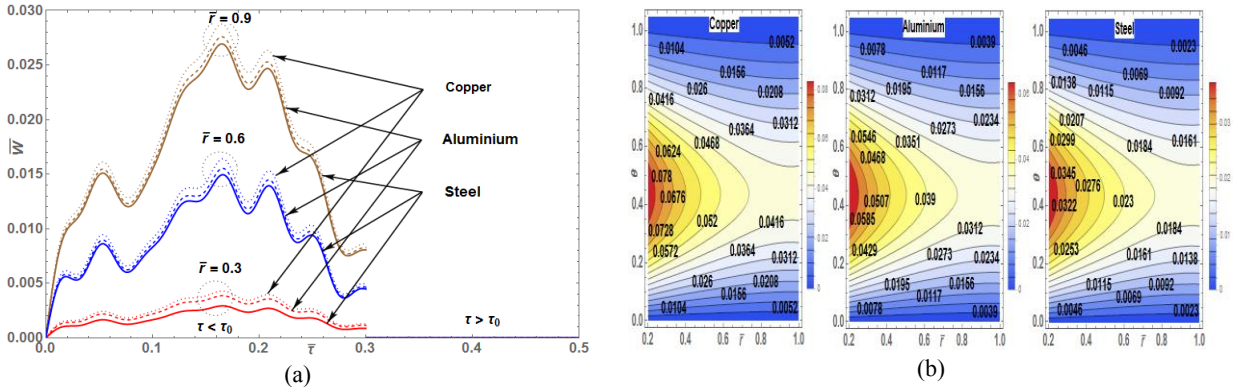

(a) (b)

Fig.3

a) Thermal deflection along time-direction for different value of $\bar{r}$. b) Contour plot of deflection along $\bar{r}\theta-$plane for a fixed value of τ.

Fig 3(a) shows thermal deflection along the time-invariant for different values of $\bar{r}$. It can be noticed that the deflection attains the maxima following a normal bell curve for every instance of the time within the range $0 \le \tau \le \tau_0$. The comprehensive peak of deflection can be observed as shown in the figure, maybe due to internal heat generation, and that varies with respect to the material properties under consideration. Fig 3(b) exhibits the thermal deflection in isolines contour plot along $\bar{r}\theta -$ plane for a fixed value of dimensionless time τ. The defection in the red area near the outer edge shows maximum displacement, maybe due to the available internal heat generation, while the dark blue colour area indicates the zero deflection at the centre of the plate. It is seen that thermal deflection is higher in the first part due to the accumulation of thermal energy available in place of ramp-type quadratic parabolic heat generation. The metals considered are steel, aluminium and copper and follows an exact relation Steel<Aluminium< Copper. The thermal deflection is shown in the contour plot shows that these values are directly proportional to their thermal diffusivity.

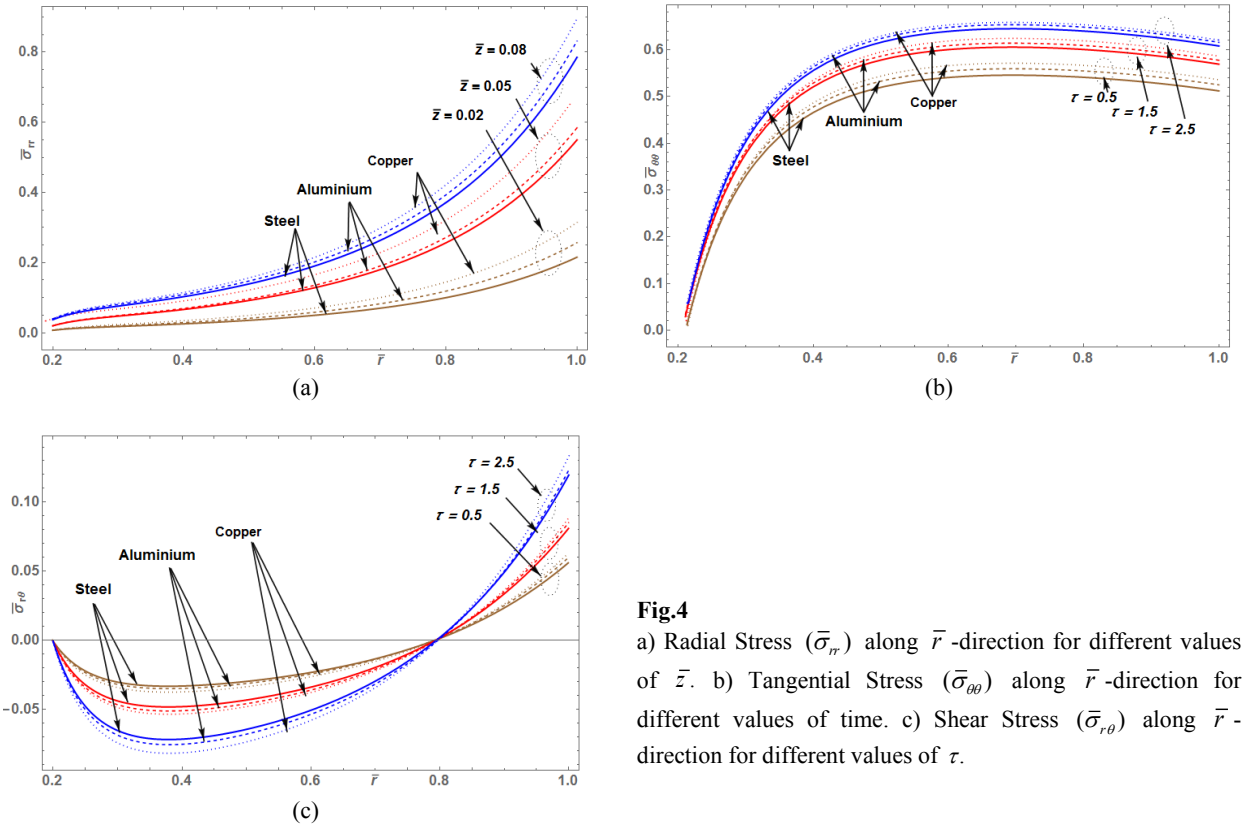

Fig.4
a) Radial Stress $(\bar{\sigma}_{rr})$ along $\bar{r}$ -direction for different values of $\bar{z}$. b) Tangential Stress $(\bar{\sigma}_{\theta\theta})$ along $\bar{r}$ -direction for different values of time. c) Shear Stress $(\bar{\sigma}_{r\theta})$ along $\bar{r}$ -direction for different values of τ.

The variation of normal stresses $\bar{\sigma}_{rr}$, $\bar{\sigma}_{\theta\theta}$ and $\bar{\sigma}_{r\theta}$ is shown in Figs.4(a), (b) and (c). Fig. 4(a) shows dimensionless radial stress along the radius of the circular plate for different thicknesses $\bar{z}$. The effect of the ramp-type heating causes the high tensile force can be easily seen at the outer edge of the thin plate, and compressive force occurs on the inner surface along the radial direction for different locations in the axial direction. This expansion and bending are in proportional to their thermal diffusivity. Fig. 4 (b) gives the analysis of dimensionless tangential stress along the radial direction at different time intervals below t_0 . It is observed from the figure that the high compressive stress occurs on the inner surface and the tensile stress appears on the inner surface along the radial direction. Fig. 4(c) displays dimensionless shear stress along the radial direction over different time intervals below t_0 . It is clear from the figure that the values of thermal shear stress decrease towards the inner part of the plate and their maximum value towards the outer part. The results obtained here are more useful in engineering problems, particularly in the determination of the state of strain in a thin circular plate. Also, any particular case of special interest can be derived by assigning suitable function $g(r,\theta)$.

5 CONCLUSIONS

In this manuscript, we have investigated the induced deflection and its associated bending stresses of the ring-type sector plate. The temperature distribution having an internal heat source is determined using the Laplace transform technique. The thermally induced deflection is obtained using an extended integral transform with the boundary condition of elastic support. The above analytical technique proposed is very straightforward and can be widely applicable in other research activity. The obtain here can be summarised as follow:

- This mathematical modelling is very efficient in handling different type of mechanical and thermal boundary condition during thermal bending analysis.
- Neglecting the inertial term in Eq. (4), the static solution for thermoelastic deflection can be obtained.
- The numerical values of the displacements and stresses for the plates of metals steel, aluminium and copper are in the proportion and follows relation Steel<Aluminium< Copper. It means these values are directly proportional to their thermal diffusivity.
- The radial and tangential stresses are observed having an increasing trend, while the shearing stress is exponentially increasing.
- The above dynamic deflection concept can be useful in predicting electro-plastic bending and other microsystem devices.

ACKNOWLEDGEMENT

The author(s) are grateful to editor and reviewers for their valuable suggestions and constructive comments which resulted in revising the paper to its present form.

APPENDIX A

The required integral transforms. The fourth-order differential equation is given as:

$$\left(\frac{\partial^2}{\partial r^2}+\frac{1}{r}\frac{\partial}{\partial r}+\frac{1}{r^2}\frac{\partial^2}{\partial \theta^2}\right)^2 f(r,\theta)=0 \tag{A.1}$$

Subjected to boundary conditions

$$\begin{aligned}\left(\frac{\partial^3}{\partial r^3}-\frac{1}{r^2}\frac{\partial}{\partial r}+\frac{1}{r}\frac{\partial^2}{\partial r^2}\right)f(r,\theta)\Big|_{r=a\,\text{or}\,b} &= -k_1 f(r,\theta)\big|_{a\,\text{or}\,b}\\ \left(\frac{\partial^2}{\partial r^2}+\frac{1}{r}\frac{\partial}{\partial r}\right)f(r,\theta)\Big|_{r=a\,\text{or}\,b} &= -k_2\frac{\partial}{\partial r}f(r,\theta)\Big|_{a\,\text{or}\,b}\end{aligned} \tag{A.2}$$

The solution of Eq. (A.1) assume to be

$$X_0(\xi r,\theta)=[A\,J_0(\xi r)+B\,Y_0(\xi r)+C\,I_0(\xi r)+D\,K_0(\xi r)]\sin m\theta \tag{A.3}$$

Applying the boundary conditions (A.2) to the above function (A.3), it reduces to matrix form, and the conditions that a solution exists to the eigenvalue equation can be given as:

$$\begin{vmatrix} \xi^3 J_1(\xi a)+k_1 J_0(\xi a) & \xi^3 Y_1(\xi a)+k_1 Y_0(\xi a) & \xi^3 I_1(\xi a)+k_1 I_0(\xi a) & \xi^3 K_1(\xi a)+k_1 K_0(\xi a)\\ -\xi J_0(\xi a)+k_2 J_1(\xi a) & -\xi Y_0(\xi a)+k_2 Y_1(\xi a) & -\xi I_0(\xi a)+k_2 I_1(\xi a) & -\xi K_0(\xi a)+k_2 K_1(\xi a)\\ \xi^3 J_1(\xi b)+k_1 J_0(\xi b) & \xi^3 Y_1(\xi b)+k_1 Y_0(\xi b) & \xi^3 I_1(\xi b)+k_1 I_0(\xi b) & \xi^3 K_1(\xi b)+k_1 K_0(\xi b)\\ -\xi J_0(\xi b)+k_2 J_1(\xi b) & -\xi Y_0(\xi b)+k_2 Y_1(\xi b) & -\xi I_0(\xi b)+k_2 I_1(\xi b) & -\xi K_0(\xi b)+k_2 K_1(\xi b) \end{vmatrix}=0 \tag{A.4}$$

and let assume that ξ_j be the positive roots of Eq. (A.4). Now the required integral transform can be obtained as:

$$\bar{f}(\xi_j,\theta)=\int_a^b\int_0^{2\pi} r f(r,\theta)\, X_0(k_1,k_2,\xi_j r,\theta)\,dr\,d\theta \tag{A.5}$$

In which kernel of the transform is taken as:

$$\begin{aligned} X_0(k_1,k_2,\xi_j r,\theta)=\{&A_j(k_1,k_2)J_0(\xi_j r)-B_j(k_1,k_2)Y_0(\xi_j r)\\ &+C_j(k_1,k_2)I_0(\xi_j r)-D_j(k_1,k_2)K_0(\xi_j r)\}\sin m\theta \end{aligned} \tag{A.6}$$

whose coefficients as the co-factor of the determinant given in Eq. (A.4) are given as:

$$\begin{aligned} A_j&=\begin{vmatrix} -\xi Y_0(\xi a)+k_2Y_1(\xi a) & -\xi I_0(\xi a)+k_2I_1(\xi a) & -\xi K_0(\xi a)+k_2K_1(\xi a)\\ \xi^3Y_1(\xi b)+k_1Y_0(\xi b) & \xi^3I_1(\xi b)+k_1I_0(\xi b) & \xi^3K_1(\xi b)+k_1K_0(\xi b)\\ -\xi Y_0(\xi b)+k_2Y_1(\xi b) & -\xi I_0(\xi b)+k_2I_1(\xi b) & -\xi K_0(\xi b)+k_2K_1(\xi b)\end{vmatrix}\\ B_j&=\begin{vmatrix} -\xi Y_0(\xi a)+k_2Y_1(\xi a) & -\xi I_0(\xi a)+k_2I_1(\xi a & -\xi K_0(\xi a)+k_2K_1(\xi a)\\ \xi^3J_1(\xi b)+k_1J_0(\xi b) & \xi^3I_1(\xi b)+k_1I_0(\xi b) & \xi^3K_1(\xi b)+k_1K_0(\xi b)\\ -\xi J_0(\xi b)+k_2J_1(\xi b) & -\xi I_0(\xi b)+k_2I_1(\xi b) & -\xi K_0(\xi b)+k_2K_1(\xi b)\end{vmatrix}\\ C_j&=\begin{vmatrix} -\xi J_0(\xi a)+k_2J_1(\xi a) & -\xi Y_0(\xi a)+k_2Y_1(\xi a) & -\xi K_0(\xi a)+k_2K_1(\xi a)\\ \xi^3J_1(\xi b)+k_1J_0(\xi b) & \xi^3Y_1(\xi b)+k_1Y_0(\xi b) & \xi^3K_1(\xi b)+k_1K_0(\xi b)\\ -\xi J_0(\xi b)+k_2J_1(\xi b) & -\xi Y_0(\xi b)+k_2Y_1(\xi b) & -\xi K_0(\xi b)+k_2K_1(\xi b)\end{vmatrix}\\ D_j&=\begin{vmatrix} -\xi J_0(\xi a)+k_2J_1(\xi a) & -\xi Y_0(\xi a)+k_2Y_1(\xi a) & -\xi I_0(\xi a)+k_2I_1(\xi a)\\ \xi^3J_1(\xi b)+k_1J_0(\xi b) & \xi^3Y_1(\xi b)+k_1Y_0(\xi b) & \xi^3I_1(\xi b)+k_1I_0(\xi b)\\ -\xi J_0(\xi b)+k_2J_1(\xi b) & -\xi Y_0(\xi b)+k_2Y_1(\xi b) & -\xi I_0(\xi b)+k_2I_1(\xi b)\end{vmatrix} \end{aligned} \tag{A.7}$$

Then the theorem of inversion can be provided in the form as:

$$f(r,\theta)=\sum_{j|\xi_j>0}^{\infty}\sum_{m=1}^{\infty}\left[\bar{f}(\xi_j,\theta)/\gamma_j\right]X_0(k_1,k_2,\xi_j r,\theta) \tag{A.8}$$

In which

$$\gamma_j=\int_a^b\int_0^{2\pi} r[X_0(k_1,k_2,\xi_j r,\theta)]^2\,dr\,d\theta$$

The fundamental operational property can be obtained as:

$$\begin{aligned} T_{X_0}\left\{\left(\frac{\partial^2}{\partial r^2}+\frac{1}{r}\frac{\partial}{\partial r}+\frac{1}{r^2}\frac{\partial^2}{\partial\theta^2}\right)^2 f(r,\theta)\right\}=&\left|r\left\{X_0(k_1,k_2,\xi_j r,\theta)\left[\left(\frac{\partial^3}{\partial r^3}-\frac{1}{r^2}\frac{\partial}{\partial r}+\frac{1}{r}\frac{\partial^2}{\partial r^2}\right)+k_1\right]f(r,\theta)\right.\right.\\ &\left.\left.-\frac{\partial X_0(k_1,k_2,\xi_j r,\theta)}{\partial r}\left[\left(\frac{\partial^2}{\partial r^2}+\frac{1}{r}\frac{\partial}{\partial r}\right)+k_2\frac{\partial}{\partial r}\right]f(r,\theta)\right\}\right|_a^b+\xi_j^4 f(\xi_j,\theta) \end{aligned} \tag{A.9}$$

Thus, we have developed an integral transformation so that it can be manipulated and solved much more easily when applied to Eq. (A.1) using the boundary conditions of the type (A.2) than in the original domain.

REFERENCES

[1] Khdeir A.A., Reddy J.N., 1991, Thermal stresses and deflections of cross-ply laminated plates using refined plate theories, *Journal of Thermal Stresses* 14(4): 419-438.

[2] Tsai H.H., Hocheng H., 1998, Analysis of transient thermal bending moments and stresses of the workpiece during surface grinding, *Journal of Thermal Stresses* **21**(6): 691-711.

[3] Kim K.S., Noda N., 2002, A Green's function approach to the deflection of Definitely FGM plate under transient thermal loading, *Archive of Applied Mechanics* **72**(127): 127-137.

[4] Na K.S., Kim J.H., 2006, Nonlinear bending response of functionally graded plates under thermal loads, *Journal of Thermal Stresses* **29**(3): 245-261.

[5] Qian H., Zhou D., Liu W., Fang H., 2014, 3-D Elasticity solutions of simply supported laminated rectangular plates in uniform temperature field, *Journal of Thermal Stresses* **37**(6): 661-677.

[6] Hasebe N., Han J.J., 2016, Green's function for infinite thin plate with elliptic hole under bending heat source and interaction between elliptic hole and crack under uniform bending heat flux, *Journal of Thermal Stresses* **39**(2): 170-182.

[7] Bhad P., Varghese V., Khalsa L., 2017, Heat source problem of thermoelasticity in an elliptic plate with thermal bending moments, *Journal of Thermal Stresses* **40**(1): 96-107.

[8] Bhad P., Varghese V., Khalsa L., 2017, A modified approach for the thermoelastic large deflection in the elliptical plate, *Archive of Applied Mechanics* **87**(4): 767-781.

[9] Bhad P., Varghese V., Khalsa L., 2017, Thermoelastic-induced vibrations on an elliptical disk with internal heat sources, *Journal of Thermal Stresses* **40**(4): 502-516.

[10] Dhakate T., Varghese V., Khalsa L., 2017, Integral transform approach for solving dynamic thermal vibrations in the elliptical disk, *Journal of Thermal Stresses* **40**(9): 1093-1110.

[11] Bhoyar S., Varghese V., Khalsa L., 2019, A method to derive thermoelastic free vibration in a simply supported annulus elliptic plate, *Journal of Thermal Stresses* **43**(2): 247-267.

[12] Mirzaei M., 2018, Thermal buckling of temperature-dependent composite super elliptical plates reinforced with carbon nanotubes, *Journal of Thermal Stresses* **41**(7): 920-935.

[13] Elsheikh A.H., Guo J., Lee K.M., 2019, Thermal deflection and thermal stresses in a thin circular plate under an axisymmetric heat source, *Journal of Thermal Stresses* **42**(3): 361-373.

[14] Marchi E., Diaz M., 1966, Elastic vibrations in the crowns of thin plates: part 1, *Atti della Accademia delle Scienze di Torino* **101**(5): 739-747.

[15] Zgrablich G., Diaz M., 1966, Elastic vibrations in crowns of thin circular plate: part 2, *Atti della Accademia delle Scienze di Torino* **101**(5): 763-770.

[16] Timoshenko S., Woinowsky-Krieger S., 1959, Theory *of Plates and Shells*, McGraw-Hill, New York.

[17] Ventsel E., Krauthammer T., 2001, *Thin Plates and Shells*, Marcel Dekker, New York.